Comput. Methods Funct. Theory
DOI 10.1007/s40315-017-0217-z

Conformal Mapping of Rectangular Heptagons II

A. B. Bogatyrev[1] · **O. A. Grigor'ev**[1]

Received: 14 January 2017 / Revised: 5 July 2017 / Accepted: 7 July 2017

Abstract A new analytical method for the conformal mapping of rectangular polygons with a straight angle at infinity to a half-plane and back is proposed. The method is based on the observation that the SC integral in this case is an abelian integral on a hyperelliptic curve, so it may be represented in terms of Riemann theta functions. The approach is illustrated by the computation of 2D-flow of ideal fluid above rectangular underlying surface and the computation of the capacities of multi-component rectangular condensers with axial symmetry.

Keywords Rectangular polygons · Schwarz–Christoffel integral · Theta functions · Conformal mapping · Jacobian

Mathematics Subject Classification 30C20 · 14H42 · 30C30

1 Introduction

Numerical methods designed to evaluate a conformal mapping from a certain "standard domain" (say, an upper half-plane) are as numerous as are their applications in the

Communicated by Darren Crowdy.

O. A. Grigor'ev was supported by RSCF Grant 16-11-10349.

✉ A. B. Bogatyrev
ab.bogatyrev@gmail.com

O. A. Grigor'ev
guelpho@mail.ru

[1] Institute for Numerical Mathematics, Russian Academy of Sciences, GSP-1, ul. Gubkina 8, Moscow 119991, Russia

Published online: 31 October 2017

area of computational physics [1]. For some domains only a finite set of parameters have to be found to substitute it into a known analytical expression for a conformal map. Delivering an example of such type of domains, rectangular polygons are the main subject of this work.

A conformal mapping from the upper half-plane to an arbitrary simply connected polygon is given by the Schwarz—Christoffel (SC) integral. If a polygon is rectangular (i.e., its angles are integer multiples of $\frac{\pi}{2}$), the SC integral is an abelian integral on a certain hyperelliptic curve. This observation, along with the well-developed function theory on Riemann surfaces, was crucial for a novel method [2–4] of evaluation of conformal maps from an upper half-plane to a rectangular polygon and back.

In a rectangular polygon, we encounter four possible junctions of the neighboring edges. They may intersect (1) at a right angle (possibly intruding); (2) at a full angle 2π (a cut); (3) at zero angle (semi-infinite "channel") and (4) at a straight angle π at infinity. The first three cases were considered in detail in the papers [3,4]; however, the remaining case—angle π at infinity—is practically important as well and requires some modification of the technique used.

As an evolution of the method represented in [3], we consider polygons containing six finite vertices and an additional one at infinity. The conformal map in question can be expressed by means of theta functions on a curve, and so does the inverse map. For the latter there exists a robust and effective method of computation [5] with controllable accuracy. Therefore, we can guarantee the machine accuracy for the conformal mapping uniformly in the polygon/half-plane.

In Sect. 2, we specify the spaces of polygons we work with. The next section is a brief summary of the theory of Riemann surfaces and theta functions relevant to our study. Section 4 describes two moduli spaces of curves we deal with in what follows. The computational algorithm is formulated in Sect. 5. In the concluding Sect. 6, we apply the obtained algorithms to the 2D-flow of ideal fluid over a rectangular surface ("city landscape"), and to the evaluation of the capacity of planar rectangular axisymmetric condensers.

2 Spaces of Polygons

We consider a simply connected heptagon with a straight angle at infinity, its sides either vertical or horizontal. Exactly three of its right angles are intruding, that is equal to $\frac{3}{2}\pi$ if measured inside the domain. The combinatorial type of the polygon is given by the sequence of indices $1 \le \sigma_1 < \sigma_2 < \sigma_3 \le 6$ of the intruding angles: the vertices $\infty =: w_0, w_1, \dots, w_6$ of the polygon are naturally ordered (see Fig. 1). We denote the space of heptagons of a given combinatorial type $\sigma = (\sigma_1, \sigma_2, \sigma_3)$ by $\mathcal{P}_\sigma$. We parametrize each space of polygons with the lengths of their sides, to which we ascribe signs for technical reasons:

$$i^s H_s := w_{s+1} - w_s, \quad s = 1, 2, \dots, 5. \tag{1}$$

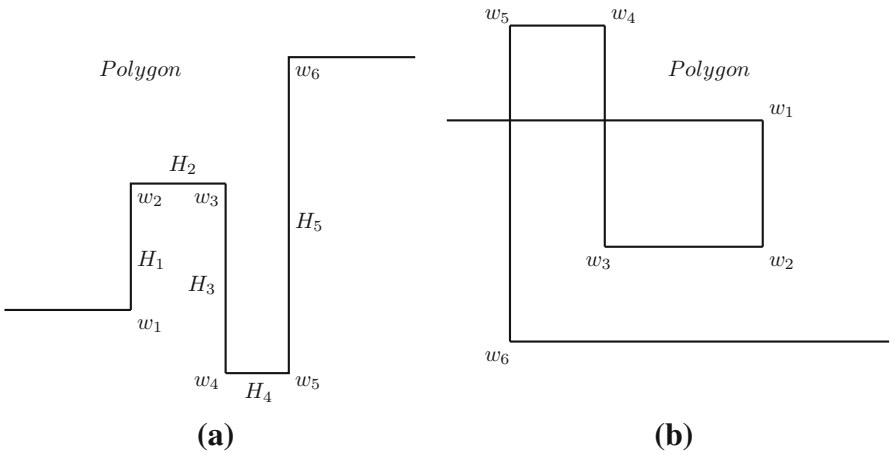

Fig. 1 **a** Polygon from the space $\mathcal{P}_{236}$. **b** Overlapping polygon from the space $\mathcal{P}_{123}$

The sign of the side length H_s is negative iff $\sigma_1 \le s < \sigma_2$ or $\sigma_3 \le s$:

$$H_s \cdot P_\sigma\left(s + \frac{1}{2}\right) < 0, \quad P_\sigma(s) := \prod_{j=1}^{3}(s - \sigma_j). \tag{2}$$

To avoid the degeneration of polygons (e.g., vanishing isthmi), we impose further restrictions on the values of H_s.

$\sigma =$	Restriction	
(126)	$H_5 - H_3 < 0$	when $H_4 - H_2 \le 0$
(156)	$H_1 - H_3 > 0$	when $H_4 - H_2 \le 0$
(123)	$H_5 < H_3$ (< 0)	
(456)	$H_1 > H_3$ (> 0)	

(3)

Note that polygons of combinatorial types $\sigma = (123)$, (234), (345) and (456)—corresponding to three consecutive right turns of the boundary—may be overlapping as in Fig. 1b.

Lemma 1 *The polygons of a given combinatorial type σ make up a connected space $\mathcal{P}_\sigma$ of real dimension* 5 *with the global coordinates H_1, H_2, H_3, H_4, H_5 subjected to the sign rule* (2) *and inequalities* (3). □

A point from a space $\mathcal{P}_\sigma$ defines a polygon up to a translation. Those translations may be eliminated when necessary by the normalization, e.g., $w_1 := 0$. The reflection in the imaginary axis induces the mapping $\mathcal{P}_{\sigma_1,\sigma_2,\sigma_3} \to \mathcal{P}_{7-\sigma_3,7-\sigma_2,7-\sigma_1,}$ which looks like $(H_1, H_2, \ldots, H_5) \to (-H_5, -H_4, \ldots, -H_1)$ in the intrinsic coordinates.

3 Hyperelliptic Curves with Six Real Branch Points

The conformal mapping of the upper half-plane to any heptagon from the space $\mathcal{P}_\sigma$ may be represented by the Schwarz–Christoffel integral. This integral can be lifted to a hyperelliptic curve with six real branch points. In this section we recall a few facts about said curves. The survey is the short version of [3, Sect. 2, 4] and does not contain any proofs, more details may be found in textbooks (cf. [6–9]).

3.1 Algebraic Model

The double cover of the sphere with six real branch points $x_1 < x_2 < \cdots < x_5 < x_6$ is a compact genus 2 Riemann surface X, the coordinates of the points in its affine part satisfying the equation

$$y^2 = \prod_{s=1}^{6}(x - x_s), \quad (x, y) \in \mathbb{C}^2. \tag{4}$$

This curve admits a *conformal involution* $J(x, y) = (x, -y)$ with six stationary points $p_s := (x_s, 0)$ and an *anticonformal involution* (*reflection*) $\bar{J}(x, y) = (\bar{x}, \bar{y})$. The stationary points set of the latter has three components known as *real ovals* of the curve. Each real oval is an embedded circle [6] and doubly covers exactly one of the segments $[x_2, x_3]$, $[x_4, x_5]$, $[x_6, x_1] \ni \infty$ of the extended real line $\hat{\mathbb{R}} := \mathbb{R} \cup \infty$. We denote those ovals as *the first, the second and the third*, respectively. The lift of the complementary set of intervals $[x_1, x_2]$, $[x_3, x_4]$, $[x_5, x_6]$ to the surface (4) gives us three *coreal ovals* which make up the set of points fixed by another anticonformal involution $\bar{J}J = J\bar{J}$.

3.2 Cycles, Differentials, Periods

We fix a special basis in the 1-homology space of the curve X intrinsically related to the latter. The first and second real ovals give us two 1-cycles, a_1 and a_2, respectively. Both cycles are oriented (up to a simultaneous change of signs) as the boundary of a pair of pants obtained by removing all real ovals from the surface. Two remaining cycles b_1 and b_2 are represented by coreal ovals of the curve oriented in such a way that the intersection matrix takes the canonical form (see Fig. 2).

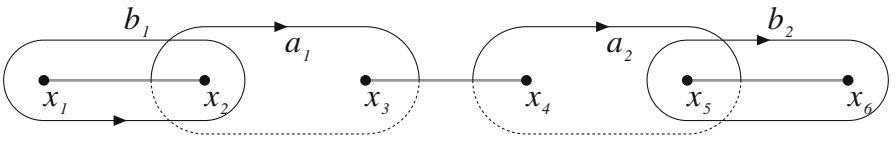

Fig. 2 Canonical basis in homologies of the curve X

The reflection of the surface acts on the aforementioned basis as follows:

$$\bar{J}a_s = a_s, \quad \bar{J}b_s = -b_s, \qquad s = 1, 2. \tag{5}$$

Holomorphic differentials on the curve X take the form

$$\mathrm{d}u_* = (C_{1*}x + C_{2*})y^{-1}\mathrm{d}x, \tag{6}$$

with C_{1*}, C_{2*} being constants. The basis of differentials dual to the basis of cycles

$$\int_{a_s} \mathrm{d}u_j := \delta_{sj}; \quad s, j = 1, 2, \tag{7}$$

determines Riemann period matrix Π with the elements

$$\Pi_{sj} := \int_{b_s} \mathrm{d}u_j; \quad s, j = 1, 2. \tag{8}$$

It is a classical result that Π is symmetric and has positive definite imaginary part [7].

From the symmetry properties (5) of the chosen basic cycles it readily follows that:

- Normalized differentials are real, i.e., $\bar{J}\mathrm{d}u_s = \overline{\mathrm{d}u_s}$, in other words, the coefficients C_* in (6) are real.
- Period matrix is purely imaginary, therefore we can introduce the symmetric and positive definite real matrix $\Omega := \mathrm{Im}(\Pi)$.

3.3 Jacobian and Abel–Jacobi Map

Definition 1 Given a Riemann period matrix Π, we define the full-rank period lattice

$$L(\Pi) = \Pi\mathbb{Z}^2 + \mathbb{Z}^2 = \int_{H_1(X,\mathbb{Z})} \mathrm{d}\boldsymbol{u}, \quad \mathrm{d}\boldsymbol{u} := (\mathrm{d}u_1, \mathrm{d}u_2)^t,$$

in $\mathbb{C}^2$ and the 4-torus $\mathrm{Jac}(X) := \mathbb{C}^2/L(\Pi)$ known as a Jacobian of the curve X.

This definition depends on the choice of the basis in the lattice $H_1(X, \mathbb{Z})$, other choices bring us to isomorphic tori.

It is convenient to represent the points $\boldsymbol{u} \in \mathbb{C}^2$ as a theta characteristic $[\boldsymbol{\epsilon}, \boldsymbol{\epsilon}']$, i.e., a couple of real 2-vectors (columns)[1] $\boldsymbol{\epsilon}, \boldsymbol{\epsilon}'$:

$$\boldsymbol{u} = \frac{1}{2}(\Pi\boldsymbol{\epsilon} + \boldsymbol{\epsilon}'). \tag{9}$$

[1] Our notation of theta characteristic as two-column vectors is not universally accepted: some authors use the transposed matrix.

The points of the Jacobian $\mathrm{Jac}(X)$ in this notation correspond to two vectors with real entries modulo 2. Second-order points of the Jacobian are represented as 2×2 matrices with binary entries 0, 1.

Definition 2 The Abel–Jacobi (briefly: AJ) map

$$\boldsymbol{u}(p) := \int_{p_1}^{p} \mathrm{d}\boldsymbol{u} \mod L(\Pi), \qquad p_1 := (x_1, 0); \quad \mathrm{d}\boldsymbol{u} := (\mathrm{d}u_1, \mathrm{d}u_2)^t, \tag{10}$$

is a correctly defined mapping from the surface X to its Jacobian.

From the Riemann–Roch formula [7] it easily follows that the Abel–Jacobi map is a holomorphic embedding of the curve into its Jacobian. In Sect. 3.4 we give an explicit equation for the image of the genus two curve in its Jacobian. Let us compute the images of the branching points $p_s = (x_s, 0)$, $s = 1, \ldots, 6$, of the curve X in the table below, where Π^s and E^s are the sth columns of the period and identity matrix, respectively. One can notice that the vector $\boldsymbol{\epsilon}(\boldsymbol{u}(p))$ is constant along the real ovals and $\boldsymbol{\epsilon}'(\boldsymbol{u}(p))$ is constant along the coreal ovals.

p	$\boldsymbol{u}(p) \bmod L(\Pi)$	$[\epsilon, \epsilon'](\boldsymbol{u}(p))$
p_2	$\Pi^1/2$	$\left[\begin{smallmatrix}1&0\\0&0\end{smallmatrix}\right]$
p_3	$(\Pi^1 + E^1)/2$	$\left[\begin{smallmatrix}1&1\\0&0\end{smallmatrix}\right]$
p_4	$(\Pi^2 + E^1)/2$	$\left[\begin{smallmatrix}0&1\\1&0\end{smallmatrix}\right]$
p_5	$(\Pi^2 + E^1 + E^2)/2$	$\left[\begin{smallmatrix}0&1\\1&1\end{smallmatrix}\right]$
p_6	$(E^1 + E^2)/2$	$\left[\begin{smallmatrix}0&1\\0&1\end{smallmatrix}\right]$

3.4 Theta Functions on Genus Two Curves

Here we give a short introduction to the theory of Riemann theta functions adapted to genus two surfaces. Three problems related to conformal mappings will be effectively solved in terms of Riemann theta functions:

- Localization of the curve inside its Jacobian;
- Representation of the 2-sheeted projection of the curve to the sphere;
- Evaluation of the normalized abelian integrals of the second and the third kinds which appear in the canonical decomposition of the SC integral into elementary ones.

Definition 3 Let $\boldsymbol{u} \in \mathbb{C}^2$ and $\Pi \in \mathbb{C}^{2\times 2}$ be a Riemann matrix, i.e., $\Pi = \Pi^t$ and $\mathrm{Im}\,\Pi > 0$. The theta function of those two arguments is the following Fourier series:

$$\theta(\boldsymbol{u}, \Pi) := \sum_{\boldsymbol{m}\in\mathbb{Z}^2} \exp(2\pi i \boldsymbol{m}^t \boldsymbol{u} + \pi i \boldsymbol{m}^t \Pi \boldsymbol{m}).$$

Also consider theta functions with characteristics which are a slight modification of the above

$$\theta[2\boldsymbol{\epsilon}, 2\boldsymbol{\epsilon}'](\boldsymbol{u}, \Pi) := \sum_{\boldsymbol{m}\in\mathbb{Z}^2} \exp(2\pi i(\boldsymbol{m}+\boldsymbol{\epsilon})^t(\boldsymbol{u}+\boldsymbol{\epsilon}') + \pi i(\boldsymbol{m}+\boldsymbol{\epsilon})^t\Pi(\boldsymbol{m}+\boldsymbol{\epsilon}))$$
$$= \exp(i\pi\boldsymbol{\epsilon}^t\Pi\boldsymbol{\epsilon} + 2i\pi\boldsymbol{\epsilon}^t(\boldsymbol{u}+\boldsymbol{\epsilon}'))\theta(\boldsymbol{u}+\Pi\boldsymbol{\epsilon}+\boldsymbol{\epsilon}', \Pi), \quad \boldsymbol{\epsilon}, \boldsymbol{\epsilon}' \in \mathbb{R}^2.$$

The matrix argument Π of the theta function is usually omitted when it is clear which matrix is used. An omitted vector argument $\boldsymbol{u}$ is supposed to be zero and the appropriate function of Π is called the theta constant:

$$\theta[\boldsymbol{\epsilon}, \boldsymbol{\epsilon}'] := \theta[\boldsymbol{\epsilon}, \boldsymbol{\epsilon}'](0, \Pi).$$

The convergence of these series is based on the positive definiteness of Im Π. The series converges rapidly and one can approximate its value with preassigned accuracy by taking a partial sum [5]. One can easily check the following quasi-periodicity properties of the theta function with respect to the lattice $L(\Pi) := \Pi\mathbb{Z}^2 + \mathbb{Z}^2$:

$$\theta(\boldsymbol{u}+\Pi\boldsymbol{m}+\boldsymbol{m}', \Pi) = \exp(-i\pi\boldsymbol{m}^t\Pi\boldsymbol{m} - 2i\pi\boldsymbol{m}^t\boldsymbol{u})\theta(\boldsymbol{u}, \Pi), \quad \boldsymbol{m}, \boldsymbol{m}' \in \mathbb{Z}^2. \tag{11}$$

The quasi-periodicity of theta functions with characteristics is easily deduced from the last formula.

Remark 1 (i) The theta function with integer characteristics $[2\boldsymbol{\epsilon}, 2\boldsymbol{\epsilon}']$ is either even or odd depending on the parity of the inner product $4\boldsymbol{\epsilon}^t \cdot \boldsymbol{\epsilon}'$. In particular, all odd theta constants are zeros.

(ii) It is convenient to represent integer theta characteristics as the sums of AJ images of the branch points, keeping only the indices of those points: $[sk..l]$ stands for the sum modulo 2 of the theta characteristics of points $\boldsymbol{u}(p_s), \boldsymbol{u}(p_k), \ldots, \boldsymbol{u}(p_l)$, e.g., characteristics [35] corresponds to $\left[\begin{smallmatrix}10\\11\end{smallmatrix}\right]$.

3.4.1 Image of the Abel–Jacobi Map

The locus of a genus 2 curve embedded into its Jacobian may be reconstructed by solving a single equation.

Theorem 1 (Riemann) *A point $\boldsymbol{u}$ of the Jacobian lies in the image $\boldsymbol{u}(X)$ of the Abel–Jacobi map iff*

$$\theta[35](\boldsymbol{u}) = 0. \tag{12}$$

For a similar property of the image of the AJ embedding for higher genus curves see [10].

3.4.2 Projection to the Sphere

Any meromorphic function on the curve may be effectively calculated via the Riemann theta functions once we know its divisor [7,11]. For instance, take the degree 2 function $x(p)$ on the hyperelliptic curve (4). This projection is unique if fully normalized. The incomplete normalization like $x(p_j) = 0$; $x(p_0) = \infty$ brings us to a simple expression containing unspecified dilation

$$x(p) := \mathrm{Const}\frac{\theta^2[jk35](\boldsymbol{u})}{\prod_{\pm}\theta[k35](\boldsymbol{u} \pm \boldsymbol{u}^0)}, \qquad \boldsymbol{u} = \boldsymbol{u}(p), \quad \boldsymbol{u}^0 := \boldsymbol{u}(p_0) \tag{13}$$

(here k is any index from the set $\{1, \ldots, 6\}$ different from j).

3.4.3 Second- and Third-Kind Abelian Integrals

On any Riemann surface there exists a unique abelian differential of the third kind $d\eta_{pq}$ with two simple poles at the prescribed points p, q only, residues $+1$, -1, respectively, and trivial periods along all a-cycles. Differentiating with respect to the position of p, local coordinate z at the pole being fixed, we get the a-normalized differential of the second kind $\mathrm{d}\omega_{2p} = (z - p)^{-2}\mathrm{d}z +$ holomorphic form with a double pole at p. Note that the latter differential acquires a constant factor with the change of the local coordinate z at the pole. Appropriate abelian integrals have closed expressions due to Riemann, in terms of the theta functions:

$$\eta_{pq}(s) := \int_*^s \mathrm{d}\eta_{pq} = \log\frac{\theta[\boldsymbol{\epsilon}, \boldsymbol{\epsilon}'](\boldsymbol{u}(s) - \boldsymbol{u}(p))}{\theta[\boldsymbol{\epsilon}, \boldsymbol{\epsilon}'](\boldsymbol{u}(s) - \boldsymbol{u}(q))}, \quad p, q, s \in X; \tag{14}$$

$$\omega_{2p}(s) := \int_*^s \mathrm{d}\omega_{2p} = -\nabla \log\theta[\boldsymbol{\epsilon}, \boldsymbol{\epsilon}'](\boldsymbol{u}(s) - \boldsymbol{u}(p)) \cdot \frac{\mathrm{d}\boldsymbol{u}}{\mathrm{d}z}(p) \tag{15}$$

with any odd theta characteristic $[\boldsymbol{\epsilon}, \boldsymbol{\epsilon}']$, say $[3] = [\boldsymbol{u}(p_3)]$; the gradient is taken with respect to the vector argument of the theta function. The tangent vector $\mathrm{d}\boldsymbol{u}/\mathrm{d}z(p)$ to the curve X embedded into its Jacobian is orthogonal to $\nabla\theta[35](\boldsymbol{u}(p))$ according to (12), so the second-kind integral in (15) may also be rewritten as the determinant of a 2×2 matrix.

4 Two Moduli Spaces

We are going to describe the space of the SC integrals corresponding to the rectangular polygons from the spaces $\mathcal{P}_\sigma$. This space is an extension of the underlying space of genus 2 curves with real branch points.

4.1 Genus 2 Curves with Three Real Ovals

Definition 4 The moduli space $\mathcal{M}_2\mathbb{R}_3$ is the quotient space of the cyclically ordered sextuples of points $(x_1, \ldots, x_6) \in \hat{\mathbb{R}}$ modulo the action of $\mathrm{PSL}_2(\mathbb{R})$ (i.e., real projective transformations of the equator $\hat{\mathbb{R}}$ preserving its orientation).

Taking the algebraic model (4) into account, the above definition of the moduli space is equivalent to the following [3]: moduli space $\mathcal{M}_2\mathbb{R}_3$ is the space of genus two Riemann surfaces with a reflection and three enumerated real ovals. Two surfaces are equivalent iff there is a conformal 1–1 mapping between them commuting with the reflections and respecting the marking of real ovals.

Normalizing the branch points, e.g., as $x_4 = \infty$, $x_5 = -1$, $x_6 = 0$, one gets the global coordinate system on the moduli space $\mathcal{M}_2\mathbb{R}_3$:

$$0 < x_1 < x_2 < x_3 < \infty.$$

Other normalizations bring us to other global coordinate systems in the same space. Yet another global coordinate system in this space is related to the periods of holomorphic differentials.

Theorem 2 [3] *The period mapping $\Omega(X)$ introduced in Sect. 3.2 is a real analytic diffeomorphism from the moduli space $\mathcal{M}_2\mathbb{R}_3$ to the trihedral cone*

$$0 < \Omega_{12} < \min(\Omega_{11}, \Omega_{22}). \tag{16}$$

Remark 2 The mappings from the period matrices to the (suitably normalized) set of branch points of the curve and back are effective. For genus two, it is implemented by the Rosenhain formulas [12] (see Sect. 3.4) in terms of the theta constants.

4.2 Curves with a Marked Point on a Real Oval

The problems of conformal mapping use a slightly more sophisticated moduli space, namely that of the genus two real curves with a marked point on a real oval (see e.g., [13]).

Definition 5 By $\mathcal{M}_{2,1}\mathbb{R}_3$ we mean the equivalence classes of seven cyclically ordered points $(x_0, x_1, \ldots, x_6)$ in the real equator $\hat{\mathbb{R}}$ of the Riemann sphere modulo the action of $\mathrm{PSL}_2(\mathbb{R})$ and call it the large moduli space for brevity.

An argument similar to that in the previous subsection shows that we can interpret the latter space as the space of genus two Riemann surfaces with three enumerated real ovals and a marked point $p_0 \neq Jp_0$ on the third oval. Two surfaces are equivalent iff there is a conformal mapping between them commuting with the reflections and respecting the enumeration of the ovals as well as the marked point. In Definition 5, the projection of the marked point to the sphere is designated as x_0, other coordinates $x_1, \ldots, x_6$ are the projections of the branch points of the curve. The moduli space

$\mathcal{M}_{2,1}\mathbb{R}_3$ has a natural projection to the space $\mathcal{M}_2\mathbb{R}_3$ given by forgetting the marked point x_0.

One can introduce several coordinate systems on $\mathcal{M}_{2,1}\mathbb{R}_3$. Fixing three points out of seven, say $x_4 := \infty$, $x_5 := -1$, $x_6 := 0$, the positions of the remaining four points of the 7-tuple will give us the global coordinate system on the moduli space:

$$0 < x_0 < x_1 < x_2 < x_3 < \infty. \tag{17}$$

Other normalizations of the 7-tuple of points result in different coordinate systems on the moduli space. It is a good exercise to show that the arising coordinate change is a real analytic 1–1 mapping from the 4D cone (17) to the appropriate cell.

Yet another coordinate system on $\mathcal{M}_{2,1}\mathbb{R}_3$ is the modification of that related to the periods matrix. Three variables $\Omega_{11}, \Omega_{12}, \Omega_{22}$ are inherited from the space $\mathcal{M}_2\mathbb{R}_3$ and the fourth is either u_1^0 or u_2^0, the component of the image of the marked point under the AJ map. The integration path for $\boldsymbol{u}(p_0)$ is the interval of the third real oval avoiding the branch point p_6.

Lemma 2 [3] *Each mapping* $(x_0, x_1, x_2, x_3) \to (\Omega_{11}, \Omega_{12}, \Omega_{22}, u_s^0)$, $s = 1, 2$, *is a real analytic diffeomorphism of the cone* (17) *to the product of the cone* (16) *and the interval* $I/2$, $I := (0, 1)$.

4.3 Schwarz–Christoffel Differentials

Given an element of the large moduli space represented by the 7-tuple $\infty =: x_0, x_1, \ldots, x_6$ and a three element subset σ of $\{1, \ldots, 6\}$ as before, consider the following abelian differential:

$$\mathrm{d}w_\sigma = \mathsf{A} P_{X,\sigma}(x)\frac{\mathrm{d}x}{y}, \qquad P_{X,\sigma}(x) := \prod_{j\in\sigma}(x - x_j), \quad \mathsf{A} > 0, \tag{18}$$

where $y^2 = \prod_{j=1}^6 (x - x_j)$. It is called *the Schwarz–Christoffel differential*. It is real, odd with respect to the conformal involution J of the curve and determined intrinsically up to a dilation by the divisor (the set of zeros and poles) $(\mathrm{d}w_\sigma) = 2(\sum_{j\in\sigma} p_j - p_0 - Jp_0)$.

Each polygon from the space $\mathcal{P}_\sigma$ is the image of the upper half-plane under the suitable Schwarz–Christoffel map

$$w_\sigma(x) := \int_*^x \mathrm{d}w_\sigma. \tag{19}$$

Here, we have used a natural embedding of the upper half-plane $\mathbb{H}$ into the curve $X \in \mathcal{M}_{2,1}\mathbb{R}_3$ with a marked point on the real oval. The total lift $x^{-1}\mathbb{H} \subset X$ has two components and exactly one of them has the marked point p_0 on its boundary.

Slightly modifying the proof of a similar theorem considering rectangular heptagons with one zero angle vertex at infinity [3], we obtain the following result.

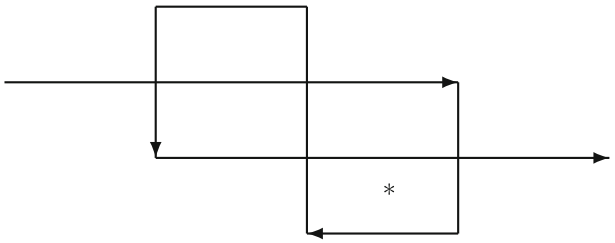

Fig. 3 Impossible image of the real line under w_{123} map

Theorem 3 *A Schwarz–Christoffel mapping $w_\sigma(x)$ induces a real analytic diffeomorphic map from the decorated moduli space $\mathcal{M}_{2,1}\mathbb{R}_3 \times \mathbb{R}^+$ to the heptagon space $\mathcal{P}_\sigma$.*

Proof Since each SC differential (18) is real, the increment of the SC map (19) on the boundary of the disc $\mathbb{H}$ embedded into the Riemann surface X is real on the real ovals and it is purely imaginary on the coreal ovals; also it is monotonic between the branch points. The image of the boundary of $\mathbb{H}$ under the SC map is a rectangular polygonal line with the same sequence of left/right turns as in any heptagon from the space $\mathcal{P}_\sigma$.

Indeed, let us check that the coordinates H_s, $s = 1, 5$, of the polygon, defined in (1), satisfy the sign rule (2) and the restrictions (3). The differential $i^{6-s}\mathrm{d}x/y$ is positive on each segment (x_s, x_{s+1}) contained in the boundary of the upper half-plane. We have a sequence of identities:

$$
\begin{aligned}
i^s H_s &:= w_{s+1} - w_s := \int_{x_s}^{x_{s+1}} \mathrm{d}w_\sigma \\
&= -i^s \mathsf{A} \int_{x_s}^{x_{s+1}} i^{6-s} P_{X,\sigma}(x) \frac{\mathrm{d}x}{y} \in -i^s \mathrm{Sgn}\ P_{X,\sigma}|_{(x_s,x_{s+1})}\ \mathbb{R}_+,
\end{aligned}
$$

which entails (2) since the sign of the polynomial $P_{X,\sigma}(x)$ on the interval (x_s, x_{s+1}) is the same as the sign of the value $P_\sigma(s + \frac{1}{2})$. The restrictions (3) hold, e.g., for the topological reason: suppose for instance that $H_3 < H_5$ for $\sigma = (123)$, then the image of the real line under the SC map has the appearance shown in Fig. 3. According to the argument principle, each point of the rectangle marked by $*$ have (-1) preimages in $\mathbb{H}$, which is impossible.

We have established a 1–1 correspondence between the decorated moduli space and the space of heptagons induced by the SC map (19). Now we prove that the direct and the inverse mappings are real analytic. One can easily see that the dimensions of the heptagon are the half-periods of the corresponding SC integral since the differential is odd with respect to the involution J:

$$
\begin{aligned}
i H_1 &:= \int_{p_1}^{p_2} \mathrm{d}w_\sigma = \frac{1}{2} \int_{-b_1} \mathrm{d}w_\sigma; \\
i^2 H_2 &:= \int_{p_2}^{p_3} \mathrm{d}w_\sigma = \frac{1}{2} \int_{a_1} \mathrm{d}w_\sigma;
\end{aligned}
$$

$$
\begin{aligned}
i^3 H_3 :&= \int_{p_3}^{p_4} \mathrm{d}w_\sigma = \frac{1}{2}\left(2\pi i \operatorname{Res} \mathrm{d}w_\sigma|_{p_0} + \int_{b_1-b_2} \mathrm{d}w_\sigma\right);\\
i^4 H_4 :&= \int_{p_4}^{p_5} \mathrm{d}w_\sigma = \frac{1}{2}\int_{a_2} \mathrm{d}w_\sigma;\\
i^5 H_5 :&= \int_{p_5}^{p_6} \mathrm{d}w_\sigma = \frac{1}{2}\int_{b_2} \mathrm{d}w_\sigma.
\end{aligned}
\tag{20}
$$

The basic 1-cycles may be separated from the branch points of the surface, so the real analyticity of the direct map $\mathcal{M}_{2,1}\mathbb{R}_3 \times \mathbb{R}_+ \to \mathcal{P}_\sigma$ is clear. It remains to show that the map has full rank.

Let us consider the coordinate system in the large moduli space by fixing three points: $x_0 = \infty, x_{\sigma_1} = 0, x_{\sigma_2} = 1$. Assume that the SC-induced map degenerates at a point $(x_0, x_1, \ldots, x_6, \mathsf{A})$ of the decorated moduli space, then there exists a non-trivial tangent vector $\xi := \alpha \frac{\partial}{\partial \mathsf{A}} + \sum_{1=j\notin\{\sigma(1),\sigma(2)\}}^{6} \xi_j \frac{\partial}{\partial x_j}$ annihilating all the periods of the SC differential $\mathrm{d}w_\sigma$ at this point. This means that there is a meromorphic differential, namely

$$
\mathrm{d}v := \frac{\alpha}{\mathsf{A}}\mathrm{d}w_\sigma + \frac{1}{2}\sum_{1=j\notin\sigma}^{6} \xi_j \frac{\mathrm{d}w_\sigma}{x - x_j} - \frac{1}{2}\xi_{\sigma_3}\frac{\mathrm{d}w_\sigma}{x - x_{\sigma_3}}
$$

with vanishing cyclic and polar periods on the curve X. Said differential may only have poles at the infinity and the branch points of the surface, except those with indices in σ. The meromorphic function $v(x, y) := \int_{p_{\sigma_1}}^{(x,y)} \mathrm{d}v$ is then single valued on the surface and it has at most five simple poles along with triple zeros at the points p_{σ_1} and p_{σ_2} (since $\int_{p_{\sigma_1}}^{p_{\sigma_2}} \mathrm{d}v$ is half-period and hence zero). This function is identical zero and therefore the above tangent vector ξ is also zero. Hence the SC integral-induced mapping $\mathcal{M}_{2,1}\mathbb{R}_3 \to \mathcal{P}_\sigma$ has the full rank everywhere. □

The SC differential (18) can be canonically decomposed into a sum of a-normalized elementary ones:

$$
\mathrm{d}w_\sigma = A \cdot (\mathrm{d}\omega_{2p_0} - J^*\mathrm{d}\omega_{2p_0}) + B \cdot \mathrm{d}\eta_{p_0 J p_0} + C_1 \cdot \mathrm{d}u_1 + C_2 \cdot \mathrm{d}u_2, \tag{21}
$$

where $\mathrm{d}\omega_{2p}$ is an abelian differential of the second kind with a double pole at p, $\mathrm{d}\eta_{pq}$ is an abelian differential of the third kind with poles at p and q only and residues ± 1; $\mathrm{d}u_1$ and $\mathrm{d}u_2$ are holomorphic differentials. All the differentials involved are real as well as the constants A, B, C_1, C_2. It remains to perform an effective evaluation of the SC integral itself along with all the auxiliary parameters. Using Riemann's formulas (14), (15), we represent the integral of (21) in terms of the Jacobian variables

$$
\begin{aligned}
w_\sigma(\boldsymbol{u}) = A \det \| \nabla \log(\theta[3](\boldsymbol{u}^0 - \boldsymbol{u})\theta[3](\boldsymbol{u}^0 + \boldsymbol{u})),\ \nabla\theta[35](\boldsymbol{u}^0)\| \\
+ B \log \frac{\theta[3](\boldsymbol{u}^0 - \boldsymbol{u})}{\theta[3](\boldsymbol{u}^0 + \boldsymbol{u})} + C_1 u_1 + C_2 u_2,
\end{aligned}
\tag{22}
$$

where $\boldsymbol{u} := (u_1, u_2)^t = \boldsymbol{u}(p)$; $\boldsymbol{u}^0 := \boldsymbol{u}(p_0)$ and the periods matrix for theta is $i\Omega$.

5 Algorithm of Conformal Mapping

Based on the formulas introduced in the previous section, we can propose an algorithm for the conformal mapping of a heptagon to the half-plane and vice versa. First of all, given the heptagon we have to determine the corresponding point of the decorated moduli space $\mathcal{M}_{2,1}\mathbb{R}_3 \times \mathbb{R}_+$.

5.1 Auxiliary Parameters

Given coordinates of the polygon, we have to find nine real parameters: the imaginary part Ω of the period matrix, the AJ image $\boldsymbol{u}^0 := \boldsymbol{u}(p_0)$ of the marked point in the Jacobian of the curve, and four real scalars A, B, C_1, C_2. Those parameters give a solution of a system of nine real equations:

$$\mathrm{d}\theta[35](\boldsymbol{u}, i\Omega) \wedge \mathrm{d}w_\sigma(\boldsymbol{u}) = 0, \qquad \text{when } \boldsymbol{u} = \boldsymbol{u}(p_{\sigma_j}), \quad j = 1, 2, 3, \tag{23}$$

which means that the SC differential $\mathrm{d}w_\sigma$ has (double) zeros at three points p_{σ_j}

$$\theta[35](\boldsymbol{u}^0, i\Omega) = 0, \tag{24}$$

which means that the point $\boldsymbol{u}^0$ lies in the AJ image of the curve in the Jacobian and finally

$$\begin{aligned}
&2H_1 = 4\pi A\theta_2[35](\boldsymbol{u}^0, i\Omega) - 4\pi B u_1^0 - C_1\Omega_{11} - C_2\Omega_{12},\\
&2H_2 = -C_1,\\
&2H_4 = C_2,\\
&2H_5 = 4\pi A\theta_1[35](\boldsymbol{u}^0, i\Omega) + 4\pi B u_2^0 + C_1\Omega_{12} + C_2\Omega_{22},\\
&H_1 - H_3 + H_5 = \pi B,
\end{aligned} \tag{25}$$

where $\theta_j[*](\boldsymbol{u}, \ldots) := \partial\theta[*](\boldsymbol{u}, \ldots)/\partial u_j$. The last five equations specify the side lengths of the polygon and can be deduced by taking the SC integral along the real and coreal ovals and using the reciprocity laws [7,8]. We note that the values of B, C_1, C_2 can be found immediately and the dependence on A is linear. The dependence on Ω and u^0 is non-linear, though.

Lemma 3 *Let the side lengths $H_1, H_2, \ldots, H_5$ satisfy the restrictions* (3) *and the sign rule* (2) *of Lemma* 1. *Then the system of nine equations* (23)–(25) *has a unique solution satisfying $A < 0$, $2\boldsymbol{u}^0 \in I \times I$, $I = (0, 1)$ and Ω lying in the trihedral cone* (16).

Proof sketch Existence and uniqueness of the solution to (23)–(25) in the specified domain follows from the existence and the uniqueness of the conformal mapping of a given heptagon to the upper half-plane. □

The strategy for the solution of the auxiliary set of equations (23)–(25) by the parametric Newton method is discussed in [3].

5.2 Mapping Heptagon to the Half-Plane and Back

Here we describe (somewhat sketchy, more details may be found in [3]) the algorithm of the conformal mapping of a fixed heptagon from the space $\mathcal{P}_\sigma$ to the upper half-plane and back. First we solve the system (23)–(25) of the auxiliary equations—once for a given heptagon. Suppose a point w^* lies in the heptagon normalized by the condition $w_1 = 0$, we consider a system of two complex equations:

$$\begin{aligned} w_\sigma(\boldsymbol{u}^*) &= w^*, \\ \theta[35](\boldsymbol{u}^*, i\Omega) &= 0, \end{aligned} \tag{26}$$

with respect to the unknown complex 2-vector $\boldsymbol{u}^*$. Following arguments provided in [3], we assert that (26) has the unique solution $\boldsymbol{u}^*$ with a theta characteristic from the block $\left[\begin{smallmatrix} -I & I \\ -I & I \end{smallmatrix}\right]$, $I := (0, 1)$. It is clear from the reflection principle for conformal mappings that the set of two equations (26) may have multiple solutions. We use the theta characteristic to single out the unique one.

Substituting the solution $\boldsymbol{u}^*$ to the right-hand side of the expression (13), we get the evaluation of the conformal mapping $x(w)$ of the heptagon to the half-plane with normalization $w_j, w_l, w_0 \to 0, 1, \infty$ at the point w^*:

$$x^* = \pm \frac{\theta^2[lk35](\boldsymbol{u}^0)}{\theta^2[lkj35]} \frac{\theta^2[jk35](\boldsymbol{u}^*)}{\prod_\pm \theta[k35](\boldsymbol{u}^* \pm \boldsymbol{u}^0)}, \quad k \neq j < l. \tag{27}$$

The sign $\pm$ in the latter formula is $(-1)^{\boldsymbol{\epsilon}(l)\boldsymbol{\epsilon}'(j)}$, where $[\boldsymbol{\epsilon}(s), \boldsymbol{\epsilon}'(s)]$ is the theta characteristic corresponding to the point $\boldsymbol{u}(p_s)$.

Conversely, given a point x^* in the upper half-plane we solve a system of two equations (27) and (12) with respect to a complex 2-vector $\boldsymbol{u}^*$ with characteristics from the block mentioned above. Then we substitute this solution to the formula (22) for the SC integral in Jacobian variables to get the image w^* of the point x^* in the heptagon.

6 Applications

One can enlarge the stock of heptagonal domains at the cost of minor complication of the involved moduli spaces and the algorithm. Suppose three equations (23) are not satisfied and the zeros of the SC differentials have moved to the neighboring real or coreal ovals. Then the composite function $w_\sigma(\boldsymbol{u}(x))$ maps the upper half-plane to a heptagon with vertical or horizontal cuts emanating from the intruding right angles. The spaces of the decagons of this kind—with six right angles, three full angles (spikes) and one straight angle at infinity have dimension 8 and the corresponding conformal mappings to the half-plane use the moduli space of real genus 2 curves with four marked points on their (co)real ovals. The parametric representation for the mapping itself is the same as above, but it contains extra auxiliary parameters and equations to determine them. Now we have three more unknown points—the zeros of the SC differential—in the Jacobian, represented by six real values and satisfying six more

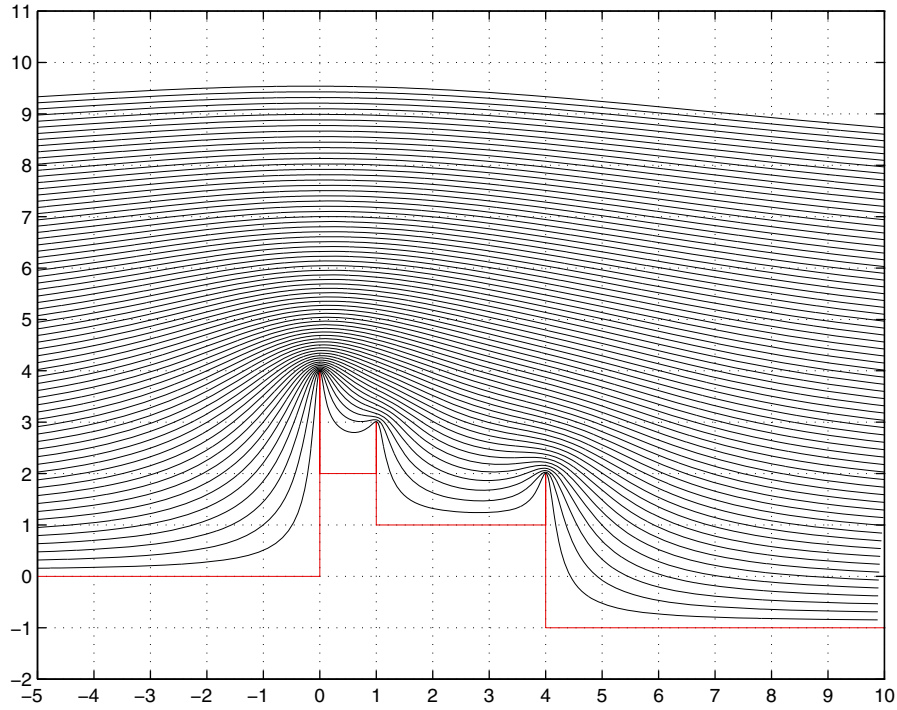

Fig. 4 Global behavior of the stream lines over the polygon from $\mathcal{P}_{235}$ with additional cuts

real equations. Three of those equations mean the same as (24): additional points lie in the AJ images of (co)real ovals of the curve. Another three equations specify the lengths of three cuts. Note that six additional variables do not participate in the final parametric representation of the conformal mapping explicitly; however, they influence the values of the auxiliary parameters involved. We hope that a motivated reader will easily reconstruct the aforementioned set of 15 equations (the majority of them linear) for 15 unknowns.

6.1 A Wind Over the City

The stream lines of the ideal fluid potential flow over a flat surface are just the horizontal straight lines. Now consider a conformal map of the upper half-plane to the decagon modeling the city landscape, with hydrodynamic normalization at infinity. The horizontal lines are thus mapped to the streamlines of a 2D ideal fluid over the surface of intricate design shown in Figs. 4 and 5.

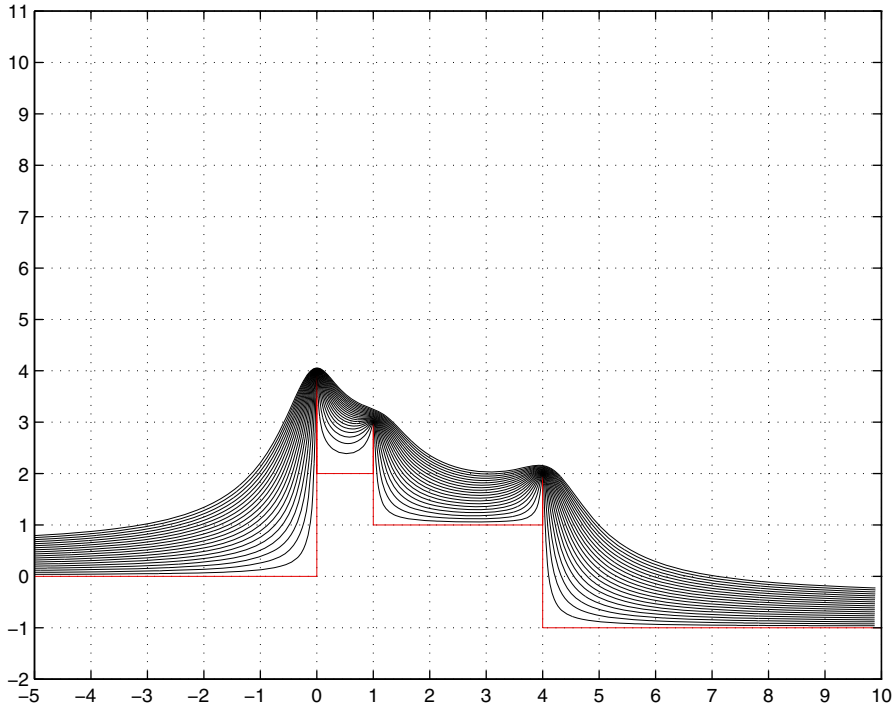

Fig. 5 Behavior of the stream lines in the vicinity the border

6.2 Calculating (Logarithmic) Capacities

Let E be a bounded compact set in the complex plane. The log capacity $C := \mathrm{Cap}(E)$ of this set is defined in terms of the asymptotic behavior of its Green's function $G_E(x)$ at infinity [14,15]:

$$G_E(x) = \log|x| - \log C + o(1), \quad x \to \infty.$$

This notion is closely related to the usual (electrotechnical) concept of capacity. Given two conductors, apply a unit voltage. The capacity of such a condenser is the charge which appears on each of the plates. This value may be also interpreted as the energy of the electric field inside the condenser or the Dirichlet integral of the electric potential. In the case that one of the plates is a circle of an increasing radius R, the other plate E being intact, the capacity of the condenser vanishes as the radius tends to infinity. However, the difference of the value inverse to the capacity and $\log R$ tends to a finite limit—the Robin constant (or Wiener capacity) of E. The exponent of the Robin constant is exactly $1/\mathrm{Cap}(E)$, as defined above.

Once we may conformally map the exterior of one set to the exterior of the other with the hydrodynamical normalization $w(x) = x + O(|x|)$, $|x| \to \infty$, the log-capacities of the two sets are equal. The exterior of an axisymmetric condenser (with all its components lying on the axis) can always be mapped to the plane with several

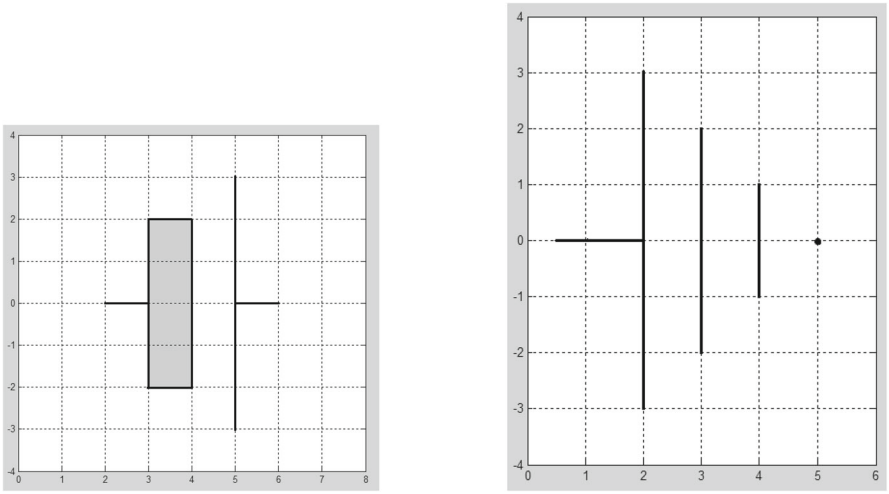

Fig. 6 Left: the capacity of "the sign of a battery" is approx. $C = 2.07891197$; right: the capacity of the "ground" sign is approx. 1.930957461

slots on a straight line. The capacity of the latter condenser may be found explicitly, say by the Akhiezer or Sebbar–Falliero formulas. For the general formula of this type of condensers in terms of theta functions see [16]. In this way one can compute the capacities of the "battery" and the "ground" symbols familiar to any electrical engineer. The dimensions of the condensers are shown in the Fig. 6.

Computed by means of different numerical techniques, capacities of rectangular domains provide an opportunity to compare the reliability of those techniques, albeit indirectly.

References

1. Trefethen, L.N., Driscoll, T.A.: Schwarz–Christoffel Mapping. Cambridge University Press, Cambridge (2002)
2. Bogatyrev, A., Hassner, M., Yarmolich, D.: An exact analytical-expression for the read sensor signal in magnetic data storage channels. In: Bruen, A.A., Wehlau, D.L. (eds.) Error-Correcting Codes, Finite Geometries and Cryptography. AMS Series Contemporary Mathematics, vol. 523, pp. 155–160. American Mathematical Society, Providence (2010)
3. Bogatyrev, A.B.: Conformal mapping of rectangular heptagons. Sbornik Math. **203**(12), 35–56 (2012)
4. Grigoriev, O.A.: Numerical-analytical method for conformal mapping of polygons with six right angles. J. Comput. Math. Math. Phys. **53**(10), 1629–1638 (2013)
5. Deconinck, B., Heil, M., Bobenko, A., van Hoeij, M., Schmies, M.: Computing Riemann theta functions. Math. Comput. **73**, 1417–1442 (2004)
6. Natanzon, S.M.: Moduli of Surfaces, Real Algebraic Curves and Their Superanalogs. AMS Translation of Mathematical Monographs, Providence (2004)
7. Farkas, H.M., Kra, I.: Riemann Surfaces. Springer, Berlin (1980)
8. Griffiths, Ph., Harris, J.: Principles of Algebraic Geometry. Wiley, New York (1978)
9. Rauch, H.E., Farkas, H.M.: Theta Functions with Applications to Riemann Surfaces. Williams & Wilkins Company, Baltimore (1974)
10. Bogatyrev, A.: Image of Abel–Jacobi map for hyperelliptic genus 3 and 4 curves. J. Approx. Theory **191**, 38–45 (2015). arXiv:1312.0445

11. Mumford, D.: Tata Lectures on Theta. I–II. Springer, Berlin (1983)
12. Rosenhain, G.: Abhandlung über die Funktionen zweier Variabeln mit vier Perioden, Mem. pres. l'Acad. de Sci. de France des savants XI (1851)
13. Bogatyrev, A.B.: Effective approach to least deviation problems. Sbornik Math. **193**(12), 1749–1769 (2002)
14. Dubinin, V.N.: Condenser Capacities and Symmetrization in Geometric Function Theory. Birkhauser, Basel (2014)
15. Goluzin, G.M.: Geometric Function Theory. AMS, Providence (1969)
16. Bogatyrev, A.B., Grigor'ev, O.A.: Closed formula for the capacity of several aligned segments. In: Complex Analysis and its Applications. Proceedings of Steklov Institute of Mathematics, vol. 298 (2017) (to appear). arXiv:1512.07154